Numerical Realizations of X-ray Computerized Tomography by Cauchy-type Boundary Integration

Hiroshi Fujiwara
Graduate School of Informatics,
Kyoto University

1 Introduction

We study numerical feasibility and properties of a Cauchy-type boundary integration formula in x-ray Computerized Tomography (CT). The integration formula has been developed by Bukhgeim et. al. [1, 2, 3] based on mainly the theory of A-analytic functions by converting the mathematical model of x-ray CT into the inverse source problem for the transport equation. However, to the best of the our knowledge, its numerical treatments have not been realized so far. It is also worthy of notice that the method has a possibility in application to the radiative transport equation [4], while the inverse Radon transform is unavailable due to its crucial dependence on straightness of x-ray propagation.

This report is based on collaborations with Professor Alexandru Tamasan (Department of Mathematics, University of Central Florida).

2 X-ray CT by the Radon Transform

Let D be a bounded and strictly convex domain with C^1 boundary in $\mathbb{R}^2$, and $\mu \in L^\infty(D)$ be its absorption coefficient. Without loss of generality, we assume that $D = \{x \in \mathbb{R}^2 \ ; \ |x| < \rho\}$ is the disk with radius ρ by letting $\mu(x) \equiv 0$ outside of the domain of interest.

The standard mathematical model of the x-ray CT [8] is to find μ satisfying the integral equation

$$\int_{x\cdot\omega=s} \mu(x)\, d\ell = R\mu(\omega, s), \tag{1}$$

from measurement of $R\mu(\omega, s)$ for all $\omega \in S^1 = \{\xi \in \mathbb{R}^2 \ ; \ |\xi| = 1\}$ and $s \in \mathbb{R}$, which is called the Radon transform of μ. Figure 1 depicts a typical measurement manner, where $R\mu(\omega, s) = R\mu(\xi^\perp, \zeta \cdot \xi^\perp)$ is the intensity of x-ray with velocity ξ emitted from $\zeta \in \partial D$. The filtered back projection (FBP) with the inverse Radon transform [9] has been well established in reconstruction of $\mu(x)$, which is given as

$$\mu(x) \approx \frac{1}{2\pi} \int_0^\pi P_\omega * h(x \cdot \omega)\, d\Omega, \qquad x \in D,$$

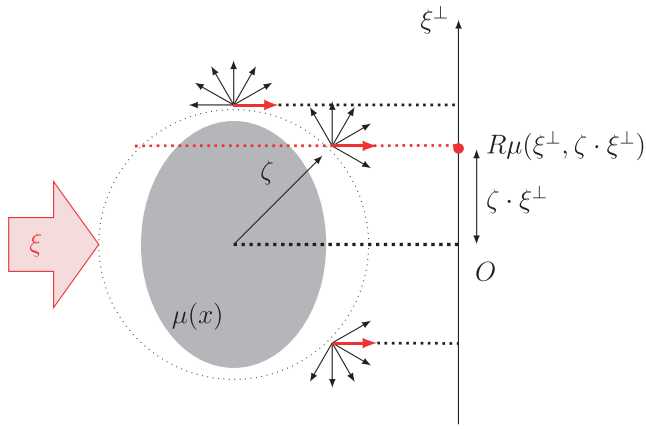

Figure 1: Mathematical Model of Measurement in X-ray Tomography

where $\Omega = \arg\omega$, $P_\omega(s) = R\mu(\omega, s)$, and $h(s)$ is a filter function whose Fourier transform approximates $|r|$.

3 Inverse Source Identification for the Transport Equation as a Mathematical Model of X-ray Tomography

In this section we summarize a mathematical model of x-ray tomography with the transport equation and its numerical algorithm developed in [2, 3, 6, 7]. Hereinafter $x = (x_1, x_2) \in \mathbb{R}^2$ is identified with $z = x_1 + ix_2 \in \mathbb{C}$ with $i = \sqrt{-1}$. Also, $\xi = (\cos\theta, \sin\theta) \in S^1$ is identified with $0 \le \theta < 2\pi$. We also assume that z denotes an interior point in Ω, while ζ indicate a boundary point on $\partial\Omega$.

Let $I(x,\xi)$, $(x,\xi) \in D\times S^1$, be the intensity of x-ray at $x \in D$ directing to ξ direction, which is induced by the incidental x-ray at $x^* \in \partial D$ with intensity $I(x^*,\xi)$. Since the boundary point $x^* \in \partial D$ is uniquely determined from $(x,\xi) \in D \times S^1$ by the law of straightness of x-ray, we introduce

$$u(x,\xi) = -\log\frac{I(x,\xi)}{I(x^*,\xi)}. \tag{2}$$

Under the notations, the mathematical model of x-ray tomography (1) is equivalent to the inverse source problem for the transport equation

$$\begin{aligned} \xi\cdot\nabla u(x,\xi) &= \mu(x), && (x,\xi) \in D\times S^1,\\ u(x,\xi) &= 0, && (x,\xi) \in \Gamma_-,\\ u(x,\xi) &= R\mu(\xi^\perp, x\cdot\xi^\perp), && (x,\xi) \in \Gamma_+, \end{aligned}$$

where $\Gamma_\pm = \{(x,\xi)\,;\, x \in \partial D, \xi \in S^1, n(x)\cdot\xi \gtrless 0\}$.

For the source identification problem, Arbuzov, Bukhgeim and Kazantsev have proposed a novel inversion algorithm based on A-analytic theory [1, 2]. The Fourier expansion of u with respect to θ is $u\big(z,\xi(\theta)\big) = \sum_{m\in\mathbb{Z}} u_m(z)e^{-im\theta}$. As the first step of the reconstruction procedure, the coefficients $u_m(\zeta)$ on the boundary ∂D are calculated from measurement data as

$$u_m(\zeta) = \frac{1}{2\pi}\int_0^{2\pi} u\big(\zeta,\xi(\theta)\big)e^{im\theta}\,d\theta, \quad m\in\mathbb{Z}. \tag{3}$$

It has been proved in [2] that $u_1(z)$ in D is obtained by the boundary integral of $u_{\mathrm{odd}}(\zeta) = \big(u_1(\zeta), u_3(\zeta), u_5(\zeta), \dots\big)$ on ∂D as

$$u_{\mathrm{odd}}(z) = \frac{1}{2\pi i}\int_{\partial D} \frac{d\zeta - S^* d\overline{\zeta}}{\overline{\zeta}-\overline{z}} \mathcal{R}\left(\frac{\zeta - z}{\overline{\zeta}-\overline{z}}\right) u_{\mathrm{odd}}(\zeta), \quad z\in D, \tag{4}$$

where $\mathcal{R}(\lambda) = (\lambda I - S^*)^{-1}$, $\lambda\in\mathbb{C}$, is the resolvent of the left translation operator $S^*(u_1,u_3,u_5,\dots) = (u_3,u_5,u_7,\dots)$. Particularly, the first Fourier mode is explicitly given in [3] as

$$u_1(z) = \frac{1}{2\pi i}\int_{\partial D}\frac{u_1(\zeta)}{\zeta - z}\,d\zeta + \frac{1}{2\pi i}\int_{\partial D}\left(\frac{d\zeta}{\zeta - z} - \frac{d\overline{\zeta}}{\overline{\zeta}-\overline{z}}\right)\left\{\sum_{p=1}^{\infty} u_{2p+1}(\zeta)\left(\frac{\overline{\zeta}-\overline{z}}{\zeta - z}\right)^p\right\}. \tag{5}$$

Finally, the attenuation μ is reconstructed as

$$\mu(x) = \mathrm{Re}\,\frac{\partial u_1}{\partial x_1}(x) + \mathrm{Im}\,\frac{\partial u_1}{\partial x_2}(x), \qquad x\in D. \tag{6}$$

In numerical reconsruction, measurement $R\mu$ is assumed to be given at $\big(\zeta_k,\xi(\theta_n)\big)\in\Gamma_+$, where $\{\zeta_k\,;\,0\le k<K\}\subset\partial D$ is K equally-spaced points on ∂D, and $\{\theta_n\,;\,0\le n<N\}\subset[0,2\pi)$ corresponds to N equally-spaced directions. We also introduce a positive integer M in order to truncate the Neumann series in (5) originated from the resolvent $\mathcal{R}$. The composite trapezoidal rule derives discretizations

$$U_{m,k} = \frac{1}{N}\sum_{n=0}^{N-1} u\big(\zeta_k,\xi(\theta_n)\big)e^{im\theta_n},$$

and

$$U_1(z) = \frac{1}{K}\sum_{k=0}^{K-1}\frac{\zeta_k}{\zeta_k - z}U_{1,k} + \frac{2}{K}\sum_{k=0}^{K-1}\mathrm{Re}\left(\frac{\zeta_k}{\zeta_k - z}\right)\left\{\sum_{3\le 2p+1\le M} U_{2p+1,k}\left(\frac{\overline{\zeta_k}-\overline{z}}{\zeta_k - z}\right)^p\right\}.$$

Since $U_1(z)$ is recovered for any $z\in D$, we can reconstruct $\mu(x)$ in D with (6) by numerical differentiations [6, 7].

4 Optimal Choice of the Truncation Parameter

In various ill-posed problems, it has been reported that "higher frequency modes" cause numerical instability and prevent reliable numerical reconstruction, whereas they are

inevitable for accurate reconstruction because they deliver information of precise structures of the system. In the present study, the Neumann series in (5) is explicitly associated with the Fourier modes. Therefore the truncation parameter M in (5) works as a regularization parameter to stabilize its numerical procedure and to control accuracy.

In order to investigate the role of M quantitatively, we demonstrate numerical examples using the modified Shepp-Logan model [10] with $K = N = 360$ and $\rho = 1.1$ [6]. Figure 2 shows the profile of the exact measurement data, where the gray region is the ellipse occupied by the Shepp-Logan model

$$E = \left\{ (x_1, x_2)\,;\ \frac{x_1^2}{0.69^2} + \frac{x_2^2}{0.92^2} < 1 \right\}$$

and the gray circle is ∂D with $\rho = 1.1$. The red curve shows measurement $u\big(\zeta, \xi(\theta)\big)$ on ∂D in the polar coordinate with respect to θ centered with $\zeta \in \partial D$ indicated by $\bullet$, and the right graph shows the magnification of that at $\zeta = (1.1, 0)$. From this measurement,

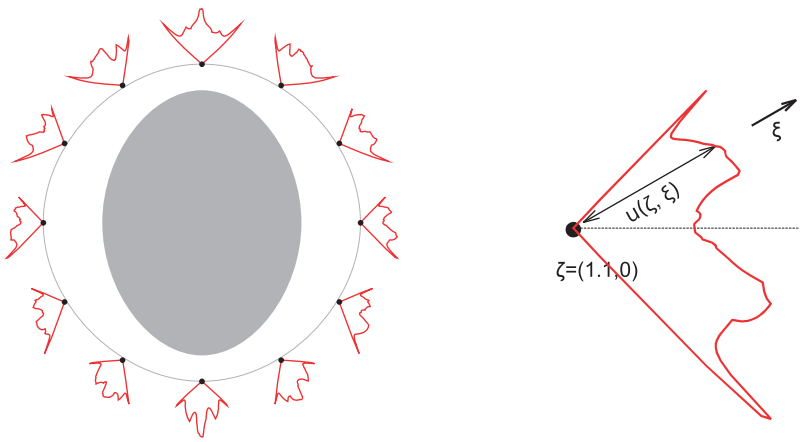

Figure 2: Exact Boundary Value $u(\zeta, \xi)$ on $\zeta \in \partial D$ of Radius $\rho = 1.1$ (left), and one at $\zeta = (1.1, 0)$ (right)

we obtain numerical reconstruction of $\mu(x)$ shown in Figure 3 by (a) the conventional FBP, and the proposed scheme with (b) $M = 30$, (c) $M = 180$, and (d) $M = 340$. In the proposed method, the parameter $M = 180$ in Figure 3(c) exhibits similar accuracy as FBP in Figure 3(a), although smaller $M = 30$ gives a blurred result in Figure 3(b). In contrast, larger $M = 340$ gives exceptional values out of the legend $0 \le \mu \le 1.2$ in Figure 3(d), which means numerical instability of the procedure.

In the present study, we propose the optimal choice of M. In a similar way as u_1, it is shown that

$$u_0(z) = \frac{1}{2\pi i} \int_{\partial D} \frac{u_0(\zeta)}{\zeta - z}\, d\zeta + \frac{1}{2\pi i} \int_{\partial D} \left(\frac{d\zeta}{\zeta - z} - \frac{d\overline{\zeta}}{\overline{\zeta} - \overline{z}} \right) \left\{ \sum_{p=1}^{\infty} u_{2p}(\zeta) \left(\frac{\overline{\zeta} - \overline{z}}{\zeta - z} \right)^p \right\},$$

which is discretized as

$$U_0(z) = \frac{1}{K} \sum_{k=0}^{K-1} \frac{\zeta_k}{\zeta_k - z} U_{0,k} + \frac{2}{K} \sum_{k=0}^{K-1} \mathrm{Re} \left(\frac{\zeta_k}{\zeta_k - z} \right) \left\{ \sum_{2 \le 2p \le M} U_{2p,k} \left(\frac{\overline{\zeta_k} - \overline{z}}{\zeta_k - z} \right)^p \right\}.$$

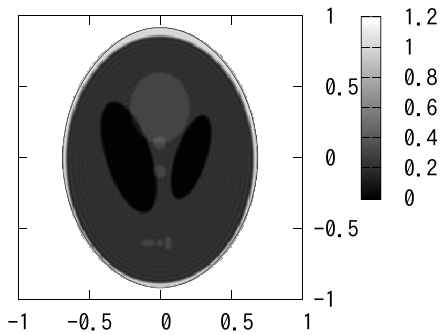

(a) Filtered Back Projection with Inverse Radon Transform

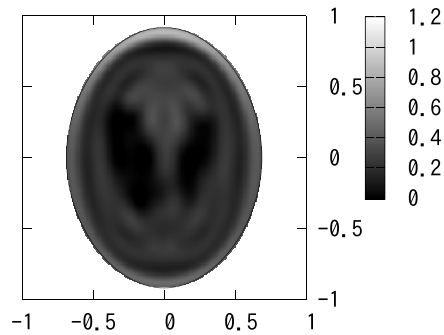

(b) Proposed Method, $M = 30$

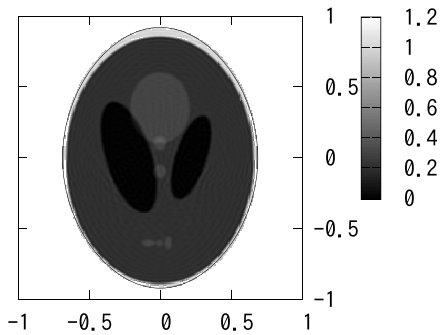

(c) Proposed Method, $M = 180$

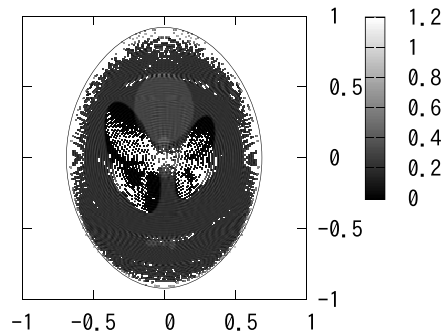

(d) Proposed Method, $M = 340$

Figure 3: Numerical Reconstructions for Modified Shepp-Logan Phantom [10] from Exact Measurement

From definition (2), u is real-valued, and hence so is u_0 from (3). Therefore, the imaginary part $\mathrm{Im}\, U_0$ obtained by numerical computation is presumed to be error which comes from discretization, rounding, and measurement.

Based on the observation, we propose the following criterion for the choice of M:

Criterion. Choose M in the reconstruction so as to minimize $\|\mathrm{Im}\, U_0\|$.

Note that The proposed criterion is practical because U_0 is computable from the measurement with fixed discretization parameters K and N.

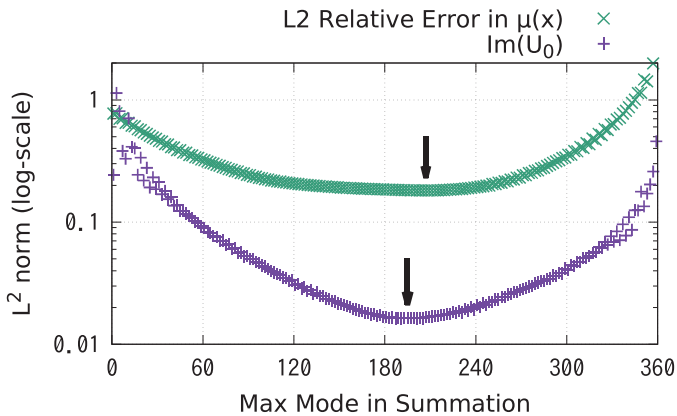

Figure 4: Choice of the Truncation Parameter M for Exact Measurement

In order to perform the criterion, we calculate $\|\mathrm{Im}\, U_0\|_2$ for $1 \leq M \leq 360$. In Figure 4, the symbols $+$ show $\|\mathrm{Im}\, U_0\|_2$ in E, while the symbols $\times$ show the relative error of reconstructed μ. The horizontal axis is $1 \leq M \leq 360$ and the vertical one is the relative L^2-norm in the logarithmic scale. In the figure, arrows indicate each minimum, $M = 195$ and $M = 207$. The proposed criterion chooses $M = 195$, and it is close to $M = 207$ which is optimal in the sense of realizing the minimal error. Furthermore, the relative errors in $M = 180$ (Figure3(c)), $M = 195$, $M = 207$ are 18.48%, 18.22%, 18.12% respectively, and significant differences cannot be observed.

5 Reconstruction from Noisy Data

In this section we show that the proposed criterion is also valid in numerical reconstruction under the presence of measurement error.

We generate the noisy data by the pseudo-random generator `normal_distribution()` in the programming language C++ with the mean 3 and 5% relative error in L^2-norm, which is depicted in Figure 5. Figure 6 shows $\|\mathrm{Im}\, U_0\|_2$ (symbols $+$) and relative errors in reconstructed μ (symbols $\times$). The former and latter are minimum at $M = 117$ and $M = 113$ in $1 \leq M \leq 360$ respectively. The proposed criterion gives $M = 117$, with which $\mu(x)$ is reconstructed shown in Figure 7. Their relative errors are 24.06% for $M = 117$ and 24.03% for $M = 113$, and the differences are insignificant. This indicate validity of the proposed parameter choice strategy.

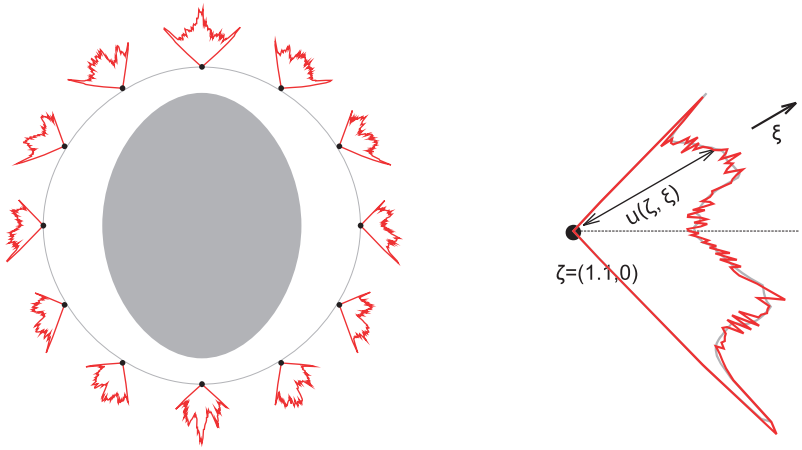

Figure 5: Measurement Data $u(\zeta, \xi)$ on $\zeta \in \partial D$ of Radius $\rho = 1.1$ with 5% Noise

6 Concluding Remarks

We have reported a numerical feasibility of x-ray tomography algorithm based on the boundary integral. In particular, parameter choice strategy has been proposed, and we demonstrate a reasonable numerical reconstruction from measurement data with errors.

Finally we announce the validity of the proposed criterion in the scattering case discussed in [4, 5], where the same boundary integral (4) plays an essential role in reconstruction. In this case, Two regularization parameters (truncation of the scattering kernel and truncation of Neumann series) are involved in the algorithm, and $\|\mathrm{Im}\, U_0\|$ also depends on them. In [5], the choice of the truncation number of the scattering kernel has been proposed for a fixed truncation number of Neumann series. On the other hand, the choice is completely compatible with the choice of the other parameter (truncation of Neumann series), and thus both can be chosen so as to minimize $\|\mathrm{Im}\, U_0\|$. Under this strategy, they gives reasonable reconstruction images similarly as this research even for the presence of measurement error.

Acknowledgments

This work was supported by JSPS KAKENHI Grant Numbers 16H02155, 18K18719, and 20H01821. A part of this work originated during the author's visit to the University of Central Florida (UCF), Orlando, Florida. The author wishes to express his gratitude to Professor Alexandru Tamasan (UCF) for his kind hospitality and valuable discussions throughout this work. The author also would like to thank the Mathematics Department at UCF for their kind hospitality.

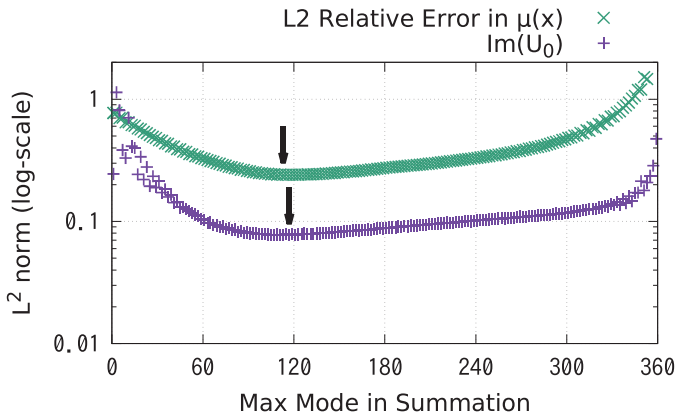

Figure 6: Regularization by the Truncation Parameter M for Measurement Data with 5% Measurement Error

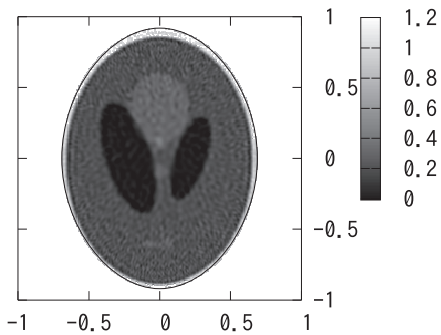

Figure 7: Numerical Examples of Reconstruction with $M = 117$, $\rho = 1.1$, and 5% Measurement Error

References

[1] E. V. Arbuzov, A. L. Bukhgeĭm, and S. G. Kazantsev, *Two-dimensional tomography problems and the theory of A-analytic functions [translation of Algebra, geometry, analysis and mathematical physics (Russian) (Novosibirsk, 1996), 6–20, 189, Izdat. Ross. Akad. Nauk Sibirsk. Otdel. Inst. Mat., Novosibirsk, 1997]*, Siberian Adv. Math., 8 (1998), pp. 1–20.

[2] A. L. Bukhgeim, *Inversion formulas in inverse problems*, in Linear Operators and Ill-Posed Problems by M. M. Lavrentiev and L. Ya. Savalev, Plenum, New York, (1995), pp. 323–378.

[3] D. V. Finch, *The attenuated X-ray transform: recent developments*, in Inside out: inverse problems and applications, vol. 47 of Math. Sci. Res. Inst. Publ., Cambridge Univ. Press, Cambridge, 2003, pp. 47–66.

[4] H. Fujiwara, K. Sadiq, and A. Tamasan, *A Fourier approach to the inverse source problem in an absorbing and non-weakly scattering medium*, Inverse Problems, 36 (2020), pp. 015005, 33.

[5] ——, *Numerical reconstruction of radiative sources in an absorbing and nondiffusing scattering medium in two dimensions*, SIAM J. Imaging Sci., 13 (2020), pp. 535–555.

[6] H. Fujiwara and A. Tamasan, *Meshless X-ray computerized tomography by the Cauchy-type integral formula*, JASCOME, 19 (2019), pp. 1–6. (in Japanese).

[7] ——, *Numerical realization of a new generation tomography algorithm based on the Cauchy-type integral formula*, Adv. Math. Sci. Appl., 28 (2019), pp. 413–424.

[8] F. Natterer and F. Wübbeling, *Mathematical methods in image reconstruction*, SIAM Monographs on Mathematical Modeling and Computation, Society for Industrial and Applied Mathematics (SIAM), Philadelphia, PA, 2001.

[9] J. Radon, *Über die bestimmung von funktionen durch ihre integralwerte längs gewisser mannigfaltigkeiten*, Berichte Sächsische Akademie der Wissenschaften zu Leipzig, Math.-Phys. Kl., 69 (1917), pp. 262–277. (translated : *On the determination of functions from their integral values along certain manifolds*, in IEEE Trans. Med. Imaging, MI-5 (1986), pp. 170–176.).

[10] P. A. Toft, *The Radon Transform — Theory and Implementation*, PhD thesis, Technical University of Denmark, 1996.